

Evaluating the V -band Photometric Metallicity with Fundamental Mode RR Lyrae in the Kepler Field

CHOW-CHOONG NGEOW¹

¹*Graduate Institute of Astronomy, National Central University, 300 Zhongda Road, 32001 Zhongli, Taiwan*

ABSTRACT

The aim of this work is to evaluate the performance of photometric metallicity $[\text{Fe}/\text{H}]$, determined based on V -band light-curves photometrically transformed from the gr -band light-curves. We tested this by using a set of homogeneous sample of fundamental mode RR Lyrae located in the *Kepler* field. It was found that the color-term is necessary in such photometric transformation. We demonstrated that including the color-term the determined photometric $[\text{Fe}/\text{H}]$ are in good agreement to the spectroscopic $[\text{Fe}/\text{H}]$, either based on the calibrated or the transformed V -band light-curves. We also tested the impact of Blazhko RR Lyrae in determining the photometric $[\text{Fe}/\text{H}]$, and found that Blazhko RR Lyrae can give consistent photometric $[\text{Fe}/\text{H}]$. Finally, we derived independent gVr -band $[\text{Fe}/\text{H}]-\phi_{31}-P$ relations (where ϕ_{31} and P are Fourier parameter and pulsation period, respectively) using our light-curves. The V -band relation is in good agreement with the most recent determination given in the literature.

1. INTRODUCTION

One of the important observed quantity, besides the pulsation periods P , for RR Lyrae is metallicity, commonly denoted as $[\text{Fe}/\text{H}]$. This is because the V -band absolute magnitude (M_V) for RR Lyrae is correlated with $[\text{Fe}/\text{H}]$. Also, $[\text{Fe}/\text{H}]$ is one of the independent parameters in the period-luminosity-metallicity (PLZ) relations (especially in the infra-red filters). For exemplary reviews on M_V - $[\text{Fe}/\text{H}]$ relation or PLZ relations, see Sandage & Tammann (2006), Beaton et al. (2018), Bhardwaj (2020), and reference therein.

The best way to measure $[\text{Fe}/\text{H}]$ is via spectroscopic observations. Errors on the spectroscopically measured $[\text{Fe}/\text{H}]$ fall in the range of ~ 0.1 to ~ 0.3 dex (e.g., see Nemeč et al. 2013), in some cases these errors can even reach to ~ 0.01 dex level (e.g., SX For in Crestani et al. 2021). However, spectroscopic observations for RR Lyrae can be expensive or time-consuming. Alternatively, $[\text{Fe}/\text{H}]$ can be estimated based on the stellar systems (for examples, in globular clusters or dwarf galaxies) or environment (for example, in Galactic halo) at which the targeted RR Lyrae are belong to. Another way to estimate $[\text{Fe}/\text{H}]$ is using light-curve properties of RR Lyrae, such as amplitudes (for examples, see

Alcock et al. 2000; Sandage 2004; Fabrizio et al. 2021) or Fourier parameter ϕ_{31} .

Since the seminal paper of Jurcsik & Kovacs (1996), who derived the $[\text{Fe}/\text{H}]-\phi_{31}-P$ relation in the V -band for ab-type (fundamental mode) RR Lyrae (hereafter RRab), a number of publications has derived a similar relation (some with additional parameters in such relation) in other filters, as well as for the c-type (first overtone) RR Lyrae. These works include: Sandage (2004) and Morgan et al. (2007) in the V -band; Smolec (2005) and Dékány et al. (2021) in the I -band; Watkins et al. (2009), Sesar et al. (2010), and Oluseyi et al. (2012) in the Sloan Digital Sky Survey (SDSS) g - and/or r -band; Nemeč et al. (2011) and Nemeč et al. (2013) in the *Kepler* K_p -band; Ngeow et al. (2016) in the R_{PTF} -band; Iorio & Belokurov (2021) in the *Gaia* G -band; Mullen et al. (2021) in the *WISE* $W1$ - and $W2$ -band; and Wu et al. (2006) for unfiltered or white-light observations. The RMS (root-mean-square) errors from these empirical relations vary from ~ 0.1 dex (Nemeč et al. 2013) to ~ 0.5 dex (in the *WISE* band, Mullen et al. 2021).

Recently, the V -band $[\text{Fe}/\text{H}]-\phi_{31}-P$ relation was updated from two works. Martínez-Vázquez et al. (2016) updated the Jurcsik & Kovacs (1996) relation by using 7 globular clusters and 8 field RR Lyrae with high-resolution spectroscopic metallicity. Furthermore, Mullen et al. (2021) re-derived the V -band $[\text{Fe}/\text{H}]-\phi_{31}-P$ relation based on a sample of $\sim 10^3$ field RRab with spectroscopic determined $[\text{Fe}/\text{H}]$. It is foreseen

that the Mullen et al. (2021) V -band relation will be widely applied in various studies on using ab-type RR Lyrae as distance tracers. On the other hand, the SDSS-like (u) $griz$ filters are becoming more popular in major synoptic sky surveys, including (but not limited to) the Pan-STARRS1 (Chambers et al. 2016), the Zwicky Transient Facility (ZTF, Bellm et al. 2019; Graham et al. 2019), the SkyMapper Southern Survey (Onken et al. 2019), the Dark Energy Survey (Dark Energy Survey Collaboration et al. 2016), the HyperSuprime-Cam Subaru Strategic Program (Aihara et al. 2018), and the Vera C. Rubin Observatory Legacy Survey of Space and Time (LSST, Ivezić et al. 2019). This implies that in order to apply the Mullen et al. (2021) V -band relation, photometric transformations need to be applied to the gr -band data from these surveys to the V -band. In principle, such transformations could add extra uncertainties to the final estimated $[\text{Fe}/\text{H}]$.

Therefore, the goal of this work is to evaluate the performance and accuracy of such photometric transformations in the derivation of photometric $[\text{Fe}/\text{H}]$, using the V -band $[\text{Fe}/\text{H}]-\phi_{31}-P$ relation. Instead of relying on inhomogeneous data taken from literature, we intended to obtain homogeneous light-curve data using the same telescope and CCD camera on the same set of RR Lyrae, such that a differential comparison can be made. We selected 30 RRab stars located in the *Kepler* field (taken from Table 7 in Nemeč et al. 2013), which possess homogeneous spectroscopic $[\text{Fe}/\text{H}]$ measured from high-resolution spectra. Section 2 describes the time-series observations of these RR Lyrae. Photometry and photometric calibration of our light-curves data are presented in Section 3. These light-curves were then used to derive their corresponding Fourier parameter ϕ_{31} as mentioned in Section 4. Performance on the photometric $[\text{Fe}/\text{H}]$ from using the V -band light-curves and the transformed light-curves are tested in Section 5. We have also derived a set of $[\text{Fe}/\text{H}]-\phi_{31}-P$ relations based on our light-curves in Section 6, followed by discussions and conclusions in Section 7. We reminded that the transmission curve for V -band filter is lied in between the g - and the r -band filters, hence we only observed our targeted RR Lyrae in these filters.

2. OBSERVATIONS AND IMAGE REDUCTION

Time-series observations of the 30 targeted RR Lyrae in the *Kepler* field were carried out using the 0.41-meter SLT telescope located at Lulin Observatory. This telescope is a $f/8.4$ Ritchey-Chrétien telescope and it is equipped with a Andor iKon-L936 CCD camera, providing a pixel scale of $0.79''/\text{pixel}$. Queue observations were

executed, via commercial software MaxIm DL and ACP Observatory Control Software, from 18 June 2019 to 24 November 2021 (weather permitted) in gVr filters. Depends on the brightness of the targeted RR Lyrae, exposure time varies between 2 to 300 second in all filters. After removing problematic images (due to bad seeings or weather, tracking problems, etc), the number of gVr sequence ranged from ~ 120 to ~ 144 for all of the 30 RR Lyrae. Subroutines in IRAF (Image Reduction and Analysis Facility; version 2.16)¹ were used to reduce these images, including bias and dark subtractions, as well as flat-fieldings. Astrometric calibration on the reduced images were done using the `astrometry.net`² (Lang et al. 2010) software suite.

3. PHOTOMETRIC CALIBRATION

For each of our targeted RR Lyrae, we constructed a reference catalog by merging the Pan-STARRS1 Data Release 1 (DR1) photometric data (Chambers et al. 2016; Flewelling et al. 2020) and the UBV photometric catalog published in Everett et al. (2012, hereafter the UBV catalog). A search area with a size of $27' \times 27'$ centered at each targeted RR Lyrae was adopted to query the Pan-STARRS1 DR1 photometric data. We applied a number of selection criteria to select only the non-varying stellar sources in the merged reference catalogs. Further details of the adopted selection criteria were given in the Appendix A. These merged reference catalogs were then cross-matched to the catalogs generated from the SExtractor³ (version 2.25.0, Bertin & Arnouts 1996) on all reduced images. The popular *MAG_AUTO* implemented in SExtractor was adopted for measuring the instrumental magnitudes. Hence, each images we have a catalog containing both of the gr -band and BV -band photometry from the Pan-STARRS1 and the UBV catalog, respectively, for the reference stars, as well as their instrumental magnitudes.

The photometric calibration was done using the following set of equations (for example, see Masci et al. 2019):

$$g^{PS1} - g^{\text{instr}} = ZP_g + C_g(g^{PS1} - r^{PS1}), \quad (1)$$

$$r^{PS1} - r^{\text{instr}} = ZP_r + C_r(g^{PS1} - r^{PS1}), \quad (2)$$

$$V - V^{\text{instr}} = ZP_V + C_V(B^{EHK} - V^{EHK}), \quad (3)$$

¹ IRAF is distributed by the National Optical Astronomy Observatories, which are operated by the Association of Universities for Research in Astronomy, Inc., under cooperative agreement with the National Science Foundation. See <https://ascl.net/9911.002>

² <https://astrometry.net/> or <https://ascl.net/1208.001>

³ <https://www.astromatic.net/software/sextractor/> or <https://ascl.net/1010.064>

where m^{PS1} or EHK are magnitudes from published catalogs (either Pan-STARRS1 or *UBV* catalog), and m^{instr} are instrumental magnitudes. An iterative 2σ -clipping linear regression, implemented in *astropy*, was used to fit these equations to determine the ZP_m and C_m coefficients.

Since our SLT observations did not include the *B* filter, we employed the photometric transformations given in [Tonry et al. \(2012\)](#) to calibrate the $(B - V)$ colors. We adopted the linear transformation between Johnson and Pan-STARRS1 photometric system from Table 6 of [Tonry et al. \(2012\)](#): $B - g^{PS1} = 0.213 + 0.587(g^{PS1} - r^{PS1})$ and $V - r^{PS1} = 0.006 + 0.474(g^{PS1} - r^{PS1})$. Then, the color transformation is found to be:

$$(B - V) = 0.207 + 1.113(g^{PS1} - r^{PS1}). \quad (4)$$

Finally, we can transform the calibrated r^{PS1} magnitudes to the *V*-band magnitude via [Tonry et al. \(2012\)](#) transformation. The transformed *V*-band magnitudes are denoted as *VT*:

$$VT = r^{PS1} + 0.006 + 0.474(g^{PS1} - r^{PS1}). \quad (5)$$

Applying equation (1) to (5) to calibrate the instrumental magnitudes requires the $(g^{PS1} - r^{PS1})$ colors of the targeted stars to be known. In case for our SLT observations with a sequence of *gVr* observations, the separation between the *gVr*-band exposures within a sequence is always less than 30 minutes (with a median of 6.2 minutes), and hence we assume the photometry obtained from the near-simultaneous *gr*-band observations is equivalent to the $(g - r)$ color at the time of observations. Combining equation (1) & (2), the instrumental colors can be calibrated to the Pan-STARRS1 photometric system via the following equation:

$$(g^{PS1} - r^{PS1}) = \frac{ZP_g - ZP_r + (g^{\text{instr}} - r^{\text{instr}})}{1 - C_g + C_r}. \quad (6)$$

The calibrated $(g^{PS1} - r^{PS1})$ colors can be applied back to equation (1) to (5) to calibrate the *grV* and *VT*-band photometry. An example of the calibrated *grV*-band and the transformed *VT*-band light-curve is shown in [Figure 1](#). All of the calibrated *grV*-band light-curves are provided in [Table 1](#). Photometric errors given in [Table 1](#) and shown in [Figure 1](#) include the errors from the instrumental magnitudes and the propagated errors from the calibration. Typical errors on $ZP_{g,r,V}$ are ~ 0.006 mag, ~ 0.004 mag, and ~ 0.013 mag, respectively. Similarly, the typical errors on $C_{g,r,V}$ are ~ 0.012 mag, ~ 0.007 mag, and ~ 0.018 mag, respectively.

4. FOURIER PARAMETERS ϕ_{31}

The *V*-band photometric $[\text{Fe}/\text{H}]$ given in [Mullen et al. \(2021\)](#) is:

$$[\text{Fe}/\text{H}]_V = -1.22[\pm 0.01] - 7.60[\pm 0.24](P - 0.58) + 1.42[\pm 0.05](\phi_{31}^s - 5.25), \quad (7)$$

with an RMS of 0.41 dex. Precise *P* for our targeted RR Lyrae are available from [Nemec et al. \(2013\)](#) based on the *Kepler* observations. Hence, we only need to determine the Fourier parameter ϕ_{31} from our calibrated *V*-band light-curves to obtain the $[\text{Fe}/\text{H}]_V$.

In general, light-curve for a periodic variable star can be fitted with an *n*-order Fourier expansion in the following form (for example, see [Petersen 1986](#); [Deb & Singh 2009](#)):

$$m(\Phi) = m_0 + \sum_{i=1}^n [a_i \cos(2\pi i \Phi) + b_i \sin(2\pi i \Phi)], \quad (8)$$

where $\Phi = t/P - INT(t/P)$ ⁴ is the pulsational phases (between 0 and 1) after folding a time-series *t* with *P*. With trigonometric identities, equation (8) can be rewritten either as a sine series or a cosine series, i.e. in the form of $m(\Phi) = m_0 + \sum_{i=1}^n A_i \sin(2\pi i \Phi + \phi_i^s)$ or $m(\Phi) = m_0 + \sum_{i=1}^n A_i \cos(2\pi i \Phi + \phi_i^c)$. Following [Simon & Lee \(1981\)](#), the Fourier parameter ϕ_{31} is either defined as $\phi_{31}^s = \phi_3^s - 3\phi_1^s$ or $\phi_{31}^c = \phi_3^c - 3\phi_1^c$, with a conversion of $\phi_{31}^c = \phi_{31}^s - \pi$ ([Ngeow et al. 2016](#)). To be consistent with [Mullen et al. \(2021\)](#), we adopted the sine series and $n = 5$ for obtaining the Fourier parameter ϕ_{31}^s . Since the error on ϕ_{31} is the same for either the sine series or the cosine series, we calculated the error on ϕ_{31}^s using the prescription given in [Petersen \(1986\)](#) and [Petersen \(1994\)](#).

For the 13 Blazhko RR Lyrae, we have also removed the modulated components following a similar procedure as described in [Ngeow et al. \(2016\)](#), in their Section 5.2; also see the reference therein), where the modulated (or Blazhko) periods, P_{BL} , were adopted from [Nemec et al. \(2013\)](#). The difference between this work and [Ngeow et al. \(2016\)](#) is we fixed $n = 5$, and only varying the (r, q) Fourier orders when fitting the modulated components. The Fourier order *r* and *q* are similar to equation (8) but for the modulated frequency $f_m = 1/P_{BL}$, and the combined frequencies $k f_0 \pm f_m$ (where

⁴ $INT(x)$ is a function that returns the integer of *x*. Normally *t* will be subtracted with a reference epoch t_0 (for example, at maximum light). For simplicity we assume $t_0 = 0$.

Table 1. *grV*-band Calibrated Light-Curves for 30 ab-Type RR Lyrae in the *Kepler* Field

KIC	HJD _{<i>g</i>}	<i>g</i>	σ_g	HJD _{<i>r</i>}	<i>r</i>	σ_r	HJD _{<i>V</i>}	<i>V</i>	σ_V
3733346	2459094.1610997790	13.131	0.038	2459094.1621529846	12.807	0.019	2459094.1616437426	13.128	0.076
3733346	2458779.0534368511	13.140	0.024	2458779.0544553185	12.767	0.013	2458779.0539576588	13.009	0.050
3733346	2458775.0634470126	13.159	0.018	2458775.0644654804	12.799	0.011	2458775.0639678198	13.072	0.026
3733346	2459019.2116095843	13.122	0.016	2459019.2126744250	12.786	0.014	2459019.2121651536	13.022	0.033
...

NOTE—Table 1 is published in its entirety in the machine-readable format. A portion is shown here for guidance regarding its form and content. HJD is the helio-Julian date at the mid-points of exposures.

Table 2. Basic Information and the Derived ϕ_{31}^s for Our Targeted RR Lyrae

KIC	P^a	P_{BL}^a	ϕ_{31}^s	ϕ_{31}^s	ϕ_{31}^s	ϕ_{31}^s	$[\text{Fe}/\text{H}]_{\text{spec}}^a$	Other Name
	(days)	(days)	(<i>g</i> -band)	(<i>r</i> -band)	(<i>V</i> -band)	(<i>VT</i> -band)	(dex)	
Non-Blazhko RR Lyrae								
3733346	0.6820264	...	4.857 ± 0.028	5.156 ± 0.028	4.941 ± 0.051	5.006 ± 0.053	−2.54 ± 0.11	NR Lyr
3866709	0.47070609	...	4.811 ± 0.028	5.107 ± 0.029	4.842 ± 0.036	4.950 ± 0.037	−1.13 ± 0.09	V715 Cyg
5299596	0.5236377	...	5.420 ± 0.030	5.840 ± 0.031	5.538 ± 0.038	5.606 ± 0.039	−0.42 ± 0.10	V782 Cyg
6070714	0.5340941	...	5.672 ± 0.030	6.090 ± 0.031	5.804 ± 0.038	5.853 ± 0.039	−0.05 ± 0.10	V784 Cyg
6100702	0.4881457	...	5.356 ± 0.018	5.706 ± 0.024	5.489 ± 0.038	5.514 ± 0.039	−0.16 ± 0.09	...
6763132	0.5877887	...	4.843 ± 0.019	5.108 ± 0.019	4.933 ± 0.041	4.969 ± 0.042	−1.89 ± 0.10	NQ Lyr
6936115	0.52739847	...	4.618 ± 0.015	4.878 ± 0.016	4.704 ± 0.030	4.750 ± 0.031	−1.98 ± 0.09	FN Lyr
7030715	0.68361247	...	5.308 ± 0.017	5.718 ± 0.020	5.452 ± 0.033	5.498 ± 0.034	−1.33 ± 0.08	...
7742534	0.4564851	...	4.627 ± 0.020	4.819 ± 0.024	4.639 ± 0.028	4.683 ± 0.029	−1.28 ± 0.20	V368 Lyr
9508655	0.5942369	...	4.894 ± 0.019	5.095 ± 0.023	5.015 ± 0.033	4.989 ± 0.034	−1.83 ± 0.12	V350 Lyr
9591503	0.5713866	...	4.857 ± 0.016	5.125 ± 0.017	4.942 ± 0.029	4.985 ± 0.030	−1.66 ± 0.12	V894 Cyg
9658012	0.533206	...	4.865 ± 0.018	5.217 ± 0.022	4.965 ± 0.026	5.032 ± 0.027	−1.28 ± 0.14	...
9717032	0.5569092	...	4.900 ± 0.041	5.099 ± 0.048	4.996 ± 0.053	5.020 ± 0.055	−1.27 ± 0.15	...
9947026	0.5485905	...	5.362 ± 0.019	5.862 ± 0.024	5.501 ± 0.036	5.576 ± 0.038	−0.59 ± 0.13	V2470 Cyg
10136240	0.5657781	...	4.863 ± 0.023	5.303 ± 0.029	4.975 ± 0.036	5.057 ± 0.037	−1.29 ± 0.23	V1107 Cyg
10136603	0.4337747	...	5.372 ± 0.016	5.676 ± 0.022	5.467 ± 0.030	5.507 ± 0.031	−0.05 ± 0.14	V839 Cyg
11802860	0.6872160	...	5.281 ± 0.017	5.519 ± 0.022	5.363 ± 0.034	5.396 ± 0.035	−1.33 ± 0.09	AW Dra
Blazhko RR Lyrae								
3864443	0.4869538	234.0	4.626 ± 0.024	4.571 ± 0.031	4.473 ± 0.041	4.577 ± 0.042	−1.66 ± 0.13	V2178 Cyg
4484128	0.5478642	92.14	4.888 ± 0.032	5.018 ± 0.036	4.861 ± 0.041	4.872 ± 0.046	−1.19 ± 0.18	V808 Cyg
5559631	0.62070001	27.667	5.251 ± 0.016	5.507 ± 0.019	5.335 ± 0.024	5.374 ± 0.025	−1.16 ± 0.11	V783 Cyg
6183128	0.561691	723.0	4.651 ± 0.026	4.933 ± 0.031	4.681 ± 0.039	4.756 ± 0.040	−1.44 ± 0.16	V354 Lyr
7198959	0.566788	39.20	4.786 ± 0.093	5.831 ± 0.088	5.273 ± 0.173	5.362 ± 0.194	−1.27 ± 0.12	RR Lyrae
7505345	0.4737027	31.05	4.584 ± 0.025	4.724 ± 0.029	4.656 ± 0.040	4.678 ± 0.044	−1.14 ± 0.17	V355 Lyr
7671081	0.5046123	123.7	4.860 ± 0.033	5.134 ± 0.042	4.771 ± 0.047	4.943 ± 0.050	−1.51 ± 0.12	V450 Lyr
9001926	0.5568016	71.6	4.917 ± 0.040	5.200 ± 0.048	4.945 ± 0.058	5.008 ± 0.061	−1.50 ± 0.20	V353 Lyr
9578833	0.5270283	62.84	5.003 ± 0.025	5.165 ± 0.031	5.084 ± 0.038	5.019 ± 0.039	−1.16 ± 0.09	V366 Lyr
9697825	0.5575765	52.07	4.884 ± 0.026	5.185 ± 0.034	4.971 ± 0.041	4.990 ± 0.042	−1.50 ± 0.29	V360 Lyr
10789273	0.48027971	54.0	4.702 ± 0.015	4.924 ± 0.017	4.795 ± 0.025	4.827 ± 0.026	−1.01 ± 0.10	V838 Cyg
11125706	0.6132200	40.23	5.478 ± 0.050	5.913 ± 0.054	5.707 ± 0.106	5.683 ± 0.114	−1.09 ± 0.08	...
12155928	0.43638507	51.999	4.618 ± 0.012	4.790 ± 0.016	4.701 ± 0.027	4.725 ± 0.028	−1.23 ± 0.15	V1104 Cyg

^a Values adopted from [Nemec et al. \(2013\)](#).

NOTE—For Blazhko RR Lyrae, the ϕ_{31}^s values were derived after the Blazhko modulations have been removed (see Section 4 for more details).

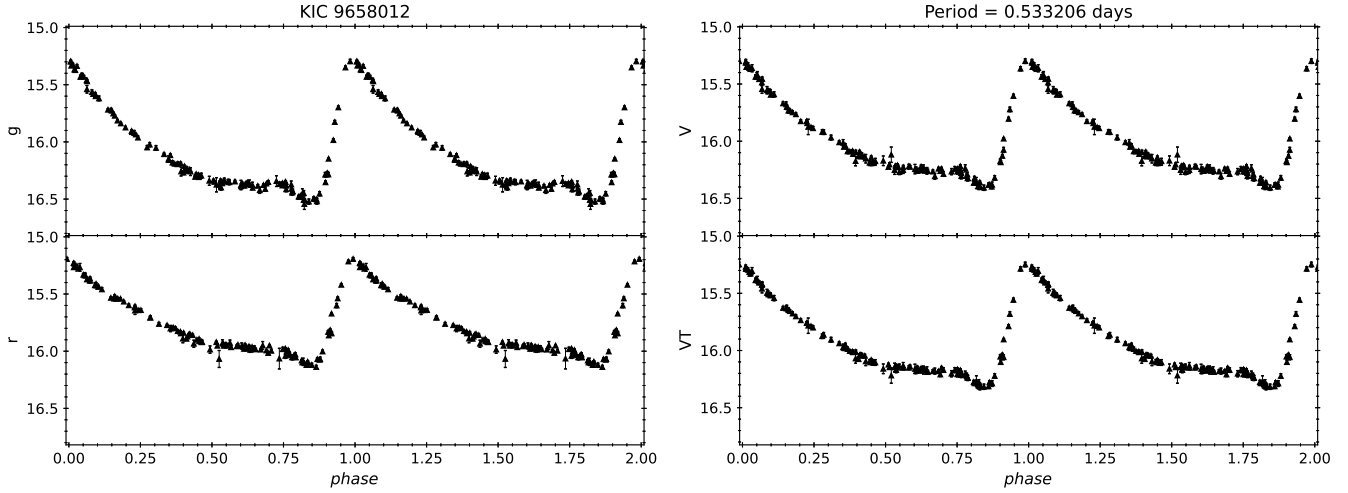
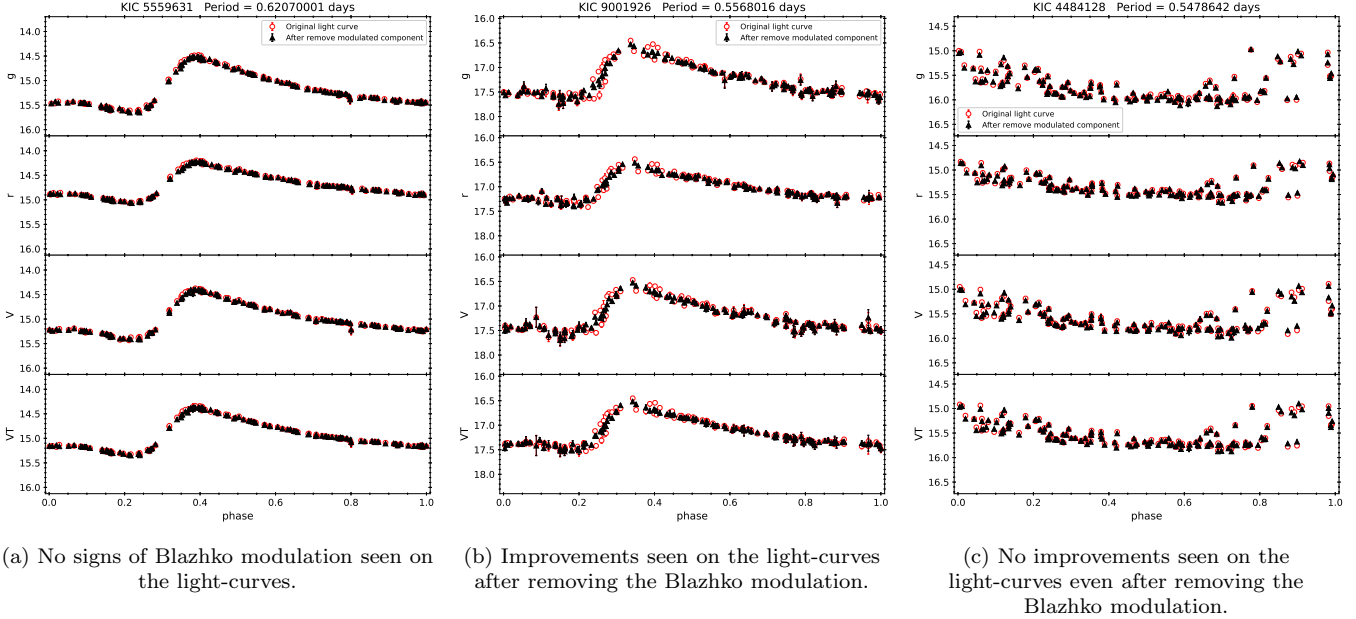


Figure 1. Calibrated *grV*-band light-curves and the transformed *VT*-band light-curve for a non-Blazhko RR Lyrae. The error bars include errors from the instrumental magnitudes and the calibration processes.



(a) No signs of Blazhko modulation seen on the light-curves.

(b) Improvements seen on the light-curves after removing the Blazhko modulation.

(c) No improvements seen on the light-curves even after removing the Blazhko modulation.

Figure 2. Example light-curves for Blazhko RR Lyrae before and after removing the Blazhko modulation. The error bars include errors from the instrumental magnitudes and the calibration processes. Panel (a) shows an example that no clear sign of Blazhko modulation seen in the light-curves. Panel (b) and (c) are examples where improvements and no improvements were seen on the light-curves after removing the Blazhko modulation, respectively.

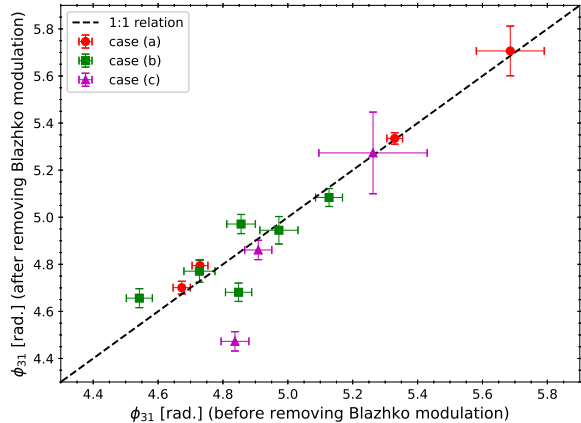


Figure 3. Comparison of the derived V -band ϕ_{31}^s Fourier parameters before and after removing the Blazhko modulations from the light curves. The filled color symbols corresponding to the three cases as presented in Figure 2. The dashed line represent the 1 : 1 relation.

$f_0 = 1/P$ is the pulsation frequency, and k is an integer runs from 0 to q), respectively. The same (r, q) Fourier orders were adopted to fit the grV and VT light-curves for a given Blazhko RR Lyrae. We found that there are four Blazhko RR Lyrae (KIC 5559631, 10789273, 11125706, and 12155928) did not show Blazhko modulation on their light-curves. In contrast, improvements can be seen on the light-curves for six Blazhko RR Lyrae (KIC 6183128, 7505345, 7671081, 9001926, 9578833, and 9697825) after removing the Blazhko modulation. The remaining three Blazhko RR Lyrae (KIC 3864443, 4484128, and 7198959) we cannot effectively remove the Blazhko modulation for a variety of (r, q) combinations. Examples of these three cases are presented in Figure 2. After removing the Blazhko modulation of the 13 Blazhko RR Lyrae (including the three RR Lyrae at which their Blazhko modulations cannot be effectively removed), we re-determined their Fourier parameter ϕ_{31}^s from the non-modulated light-curves. As an example, Figure 3 compares the V -band ϕ_{31}^s Fourier parameters before and after removing the Blazhko modulations. All of the derived ϕ_{31}^s for the 30 RR Lyrae are summarized in Table 2.

5. TESTING THE RELATION

In this Section, we test the performance of derived photometric $[\text{Fe}/\text{H}]$ from the V -band and the VT -band in several cases, assuming the spectroscopic $[\text{Fe}/\text{H}]$, $[\text{Fe}/\text{H}]_{\text{spec}}$ adopted from Nemeč et al. (2013), is the “ground truth”. Since the $[\text{Fe}/\text{H}]_{\text{spec}}$ from Nemeč et al. (2013) and the $[\text{Fe}/\text{H}]_V$ based on equation (7) are in Carretta et al. (2009) and Crestani et al. (2021) scale, respectively, we added an offset of +0.08 dex (as de-

termined in Mullen et al. 2021) to the $[\text{Fe}/\text{H}]_{\text{spec}}$ when comparing these two $[\text{Fe}/\text{H}]$ values.

We first compare the $[\text{Fe}/\text{H}]_V$ calculated from equation (7) and $[\text{Fe}/\text{H}]_{\text{spec}}$ using the calibrated or transformed light-curves, and after removing the Blazhko modulation for the Blazhko RR Lyrae, in the upper panels of Figure 4. Good agreements between $[\text{Fe}/\text{H}]_V$ and $[\text{Fe}/\text{H}]_{\text{spec}}$ can be seen from the upper left panel of Figure 4, with $\langle [\text{Fe}/\text{H}]_V - [\text{Fe}/\text{H}]_{\text{spec}} \rangle = -0.08$ dex. Similarly, photometric $[\text{Fe}/\text{H}]$ from the transformed VT -band light-curves agree well with the $[\text{Fe}/\text{H}]_{\text{spec}}$, with $\langle [\text{Fe}/\text{H}]_{VT} - [\text{Fe}/\text{H}]_{\text{spec}} \rangle = -0.01$ dex. In both cases, the standard deviations (σ) on the averaged values are $\sigma = 0.23$ dex and $\sigma = 0.24$ dex, respectively, well within the RMS of 0.41 dex given in equation (7).

Since the Blazhko periods might not be reliable determined, or might not be determined at all, for (possible) Blazhko RR Lyrae found in the synoptic time-series imaging surveys, we tested the V -band photometric $[\text{Fe}/\text{H}]$ if the Blazhko modulations were not removed on these Blazhko RR Lyrae. The middle panels of Figure 4 are similar to the upper panels, except that the Blazhko modulations were not removed. For the 13 Blazhko RR Lyrae with Blazhko modulations removed, we found $\langle [\text{Fe}/\text{H}]_V - [\text{Fe}/\text{H}]_{\text{spec}} \rangle = -0.09$ dex ($\sigma = 0.23$ dex) and $\langle [\text{Fe}/\text{H}]_{VT} - [\text{Fe}/\text{H}]_{\text{spec}} \rangle = -0.02$ dex ($\sigma = 0.25$ dex). In comparison, the averaged values changed to -0.06 dex ($\sigma = 0.26$ dex) and 0.00 dex ($\sigma = 0.29$ dex) in the V - and VT -band, respectively, if the Blazhko modulations were not removed. Nevertheless, these averaged differences (and their σ) are well within the RMS of equation (7). Therefore, it is possible to include the Blazhko RR Lyrae in estimating the V -band photometric $[\text{Fe}/\text{H}]$ without removing their Blazhko modulations. A similar conclusion was also found in Ngeow et al. (2016).

Finally, we consider an extreme case such that the Blazhko modulations were not removed for the Blazhko RR Lyrae, at the same time the color corrections were ignored (see bottom panels of Figure 4). That is, $(B - V) = 0.0$ mag and $(g^{PS1} - r^{PS1}) = 0.0$ mag in equation (3) and (5) when calibrating the V - and VT -band light-curves, hence $V = V^{\text{instr}} + ZP_V$ and $VT = r^{\text{instr}} + ZP_r + 0.006$. As a result, the VT -band light-curves are equivalent to r -band light-curves. In this case the averaged difference for the V -band photometric $[\text{Fe}/\text{H}]$ is -0.03 dex ($\sigma = 0.25$ dex), which is still reasonable to apply equation (7) to estimate the photometric $[\text{Fe}/\text{H}]$. In contrast, the VT -band photometric $[\text{Fe}/\text{H}]$ display a large offset from the 1 : 1 relation in the bottom right panel of Figure 4, with a much larger averaged difference of 0.28 dex ($\sigma = 0.28$ dex). Even

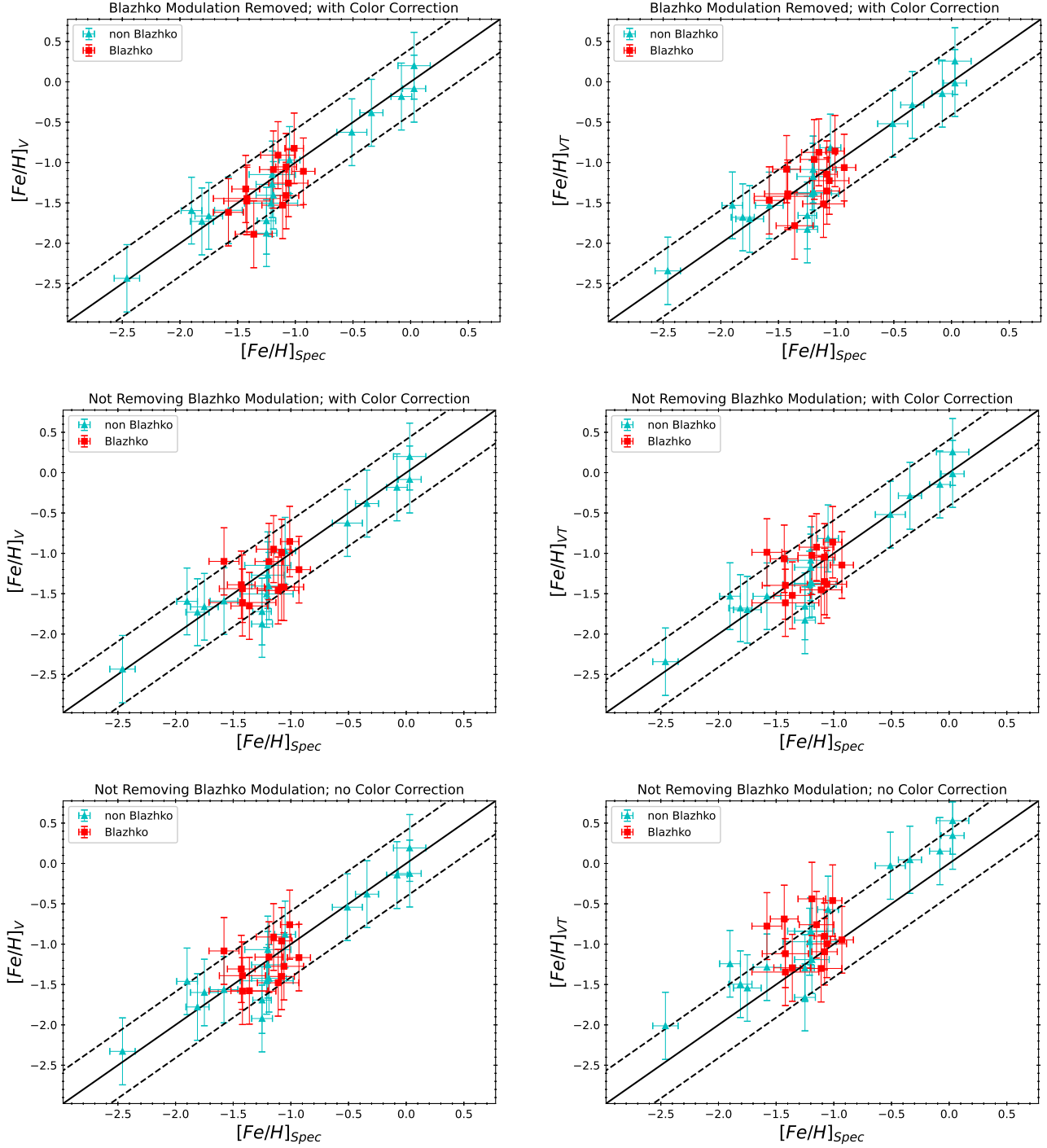


Figure 4. Comparisons of the photometric $[\text{Fe}/\text{H}]$, either in the V - (left panels) or VT -band (right panels), derived from equation (7) to the $[\text{Fe}/\text{H}]_{\text{Spec}}$. Errors on photometric $[\text{Fe}/\text{H}]$ include the RMS error and propagated errors on ϕ_{31} from equation (7), and we assume errors on P are negligible. The top, middle, and bottom panels are the comparisons for three different cases as discussed in the text (see Section 5). The solid lines represent the 1 : 1 relation and they are *not* the fits to the data. The dashed lines show the expected ± 0.41 dex RMS on the photometric $[\text{Fe}/\text{H}]$.

though this value is still within the 0.41 dex RMS of equation (7), it is large enough to induce a bias in the derived photometric $[\text{Fe}/\text{H}]$. When the color corrections were ignored or set to zero, ϕ_{31} values derived from the VT -band light curves are equivalent to those from the r -band light-curves, hence equation (7) should not be used.

Would it be possible to use a mean color when transforming the gr -band light curves to the VT -band light curves? We tested this scenario by using the mean colors for each RR Lyrae, and repeated the same procedures. In this case $\langle [\text{Fe}/\text{H}]_{VT} - [\text{Fe}/\text{H}]_{\text{spec}} \rangle = 0.28$ dex with $\sigma = 0.29$ dex. This scenario is similar to the previous case for setting the color to zero, as the constant color-term can be “absorbed” to the ZP_m , hence the VT -band light-curves would be similar to the r -band light curves. To remedy this, we provided a template color-curve in Appendix B, such that colors can be estimated at various pulsational phases using the template color-curve and an estimation of the mean color, and not assuming a constant or zero color. There are various approaches to estimate the mean color for an ab-type RR Lyrae, such as using the observed light-curves, using prior information (e.g. from other surveys or observations), using a period-color relation (e.g., in Ngeow et al. 2022), etc. It is up to the researchers to decide which approach to use, depending on their situations, needs and goals.

6. DERIVING THE RELATIONS

The Fourier parameter ϕ_{31} presented in Table 2 for all of the 30 ab-type RR Lyrae can be used to derive independent $[\text{Fe}/\text{H}]$ - ϕ_{31} - P relation in the gVr bands. Following Mullen et al. (2021), we adopted a $[\text{Fe}/\text{H}]$ - ϕ_{31} - P relation in the form of $[\text{Fe}/\text{H}] = a + b(P - P_0) + c(\phi_{31} - \phi_{31}^0)$, where P_0 and ϕ_{31}^0 are the mean period and ϕ_{31} in the sample. The zero-point (a), the period coefficient (b), and the ϕ_{31} coefficient (c) were fitted using the orthogonal distance regression (ODR) implemented in the SciPy package (i.e. `scipy.odr`), at which errors on both of the $[\text{Fe}/\text{H}]$ and ϕ_{31} were included in the fittings. The mean period for our sample is $P_0 = 0.55$ days, and the mean ϕ_{31}^0 values in the gVr -band are 4.97, 5.06, and 5.27 rad, respectively. To be consistent with Mullen et al. (2021), we adopted $P_0 = 0.58$ days and $\phi_{31}^0 = 5.25$ rad, and derived the following relations:

$$[\text{Fe}/\text{H}]_g = -1.01[\pm 0.06] - 7.43[\pm 0.80](P - 0.58) + 1.69[\pm 0.16](\phi_{31}^s - 5.25), \quad \text{RMS} = 0.24 \text{ dex}, \quad (9)$$

$$[\text{Fe}/\text{H}]_V = -1.21[\pm 0.05] - 7.67[\pm 0.78](P - 0.58) + 1.50[\pm 0.14](\phi_{31}^s - 5.25), \quad \text{RMS} = 0.24 \text{ dex}, \quad (10)$$

$$[\text{Fe}/\text{H}]_r = -1.54[\pm 0.07] - 8.28[\pm 1.04](P - 0.58) + 1.30[\pm 0.15](\phi_{31}^s - 5.25), \quad \text{RMS} = 0.30 \text{ dex}. \quad (11)$$

If we adopted P_0 and ϕ_{31}^0 from our sample, then the zero-points (a) were changed to -1.26 ± 0.04 , -1.26 ± 0.04 , and -1.27 ± 0.05 in the gVr -band, respectively. We emphasize that equation (9) to (11) are only applicable to ab-type RR Lyrae.

Similar to Nemeč et al. (2013) and Ngeow et al. (2016), we compare the predicted photometric $[\text{Fe}/\text{H}]$ derived from equation (9), (10), and (11) to the $[\text{Fe}/\text{H}]_{\text{spec}}$ in Figure 5. The Fourier parameters ϕ_{31} were adopted from Table 2, including the Blazhko RR Lyrae with Blazhko modulations being removed, when calculating the predicted photometric $[\text{Fe}/\text{H}]$. All of the three equations give $\langle [\text{Fe}/\text{H}]_{g,V,r} - [\text{Fe}/\text{H}]_{\text{spec}} \rangle = 0.0$ dex, with $\sigma_g = 0.24$ dex, $\sigma_V = 0.23$ dex, and $\sigma_r = 0.29$ dex, respectively. These standard deviations are the same or similar to the RMS given in equation (9) to (11), and no systematic offsets were seen from Figure 5.

Recall that the $[\text{Fe}/\text{H}]_{g,V,r}$ in equation (9) to (11) are in the Carretta et al. (2009) scale. If the $[\text{Fe}/\text{H}]$ were converted to the Crestani et al. (2021) scale, same as in Mullen et al. (2021), then the gVr -band zero-points (a) of the relation became -0.93 ± 0.06 , -1.13 ± 0.05 , and -1.46 ± 0.07 , respectively.

7. DISCUSSIONS AND CONCLUSIONS

In this work, we tested the performance of $[\text{Fe}/\text{H}]_V$ from Mullen et al. (2021) using a set of homogeneous ab-type RR Lyrae located in the *Kepler* field. The most important conclusion from our work is good agreement was found between $[\text{Fe}/\text{H}]_V$ and $[\text{Fe}/\text{H}]_{\text{spec}}$. This conclusion also holds if the V -band light-curves are photometrically transformed from the gr -band light-curves, as long as the color-terms are properly taken into account when calibrating the photometry. On the other hand, the transformed V -band (i.e. the VT -band) light-curves should not be used to derive $[\text{Fe}/\text{H}]_V$ if the color-terms are ignored or set to a constant. Modern synoptic time-series surveys often will not acquire near simultaneous g - and r -band photometry⁵, hence estimating the ($g-r$)

⁵ Recall that RR Lyrae are short period pulsating stars, even the g - and r -band photometry were taken in the same night but separated in few hours cannot be treated as “near simultaneous”.

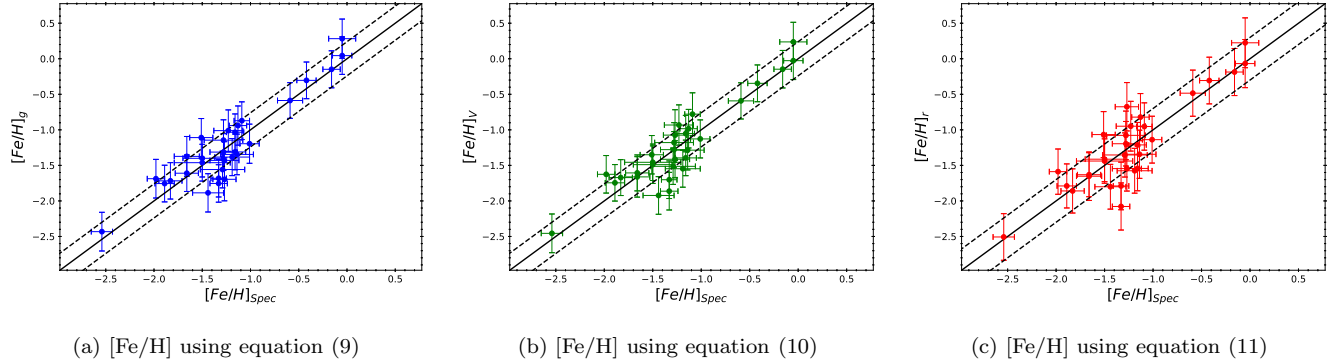


Figure 5. Comparisons of the predicted gVr -band photometric $[\text{Fe}/\text{H}]$, using equation (9), (10), and (11), to the $[\text{Fe}/\text{H}]_{\text{spec}}$ for all of the 30 ab-type RR Lyrae listed in Table 2. The solid lines are the 1 : 1 relations, and the dashed lines represent the expected RMS given in equation (9), (10), and (11).

colors at certain pulsational phases can be a non-trivial task. In Appendix B, we provide a template color-curve such that the $(g - r)$ colors can be estimated at various pulsational phases.

Our sample also contains $\sim 40\%$ Blazhko RR Lyrae, providing an opportunity to test the inclusion of Blazhko RR Lyrae in deriving $[\text{Fe}/\text{H}]_V$. Our test results suggested Blazhko RR Lyrae can be used even the Blazhko modulations are not removed. This implies RR Lyrae found in the synoptic time-series surveys (for example the LSST in coming years, see [Hernitschek & Stassun 2022](#)) can be used to determine the photometric $[\text{Fe}/\text{H}]$ without first identifying if they are Blazhko RR Lyrae or not.

Finally, we derive independent $[\text{Fe}/\text{H}]-\phi_{31}-P$ relations, for the ab-type RR Lyrae, in the gVr bands based on our data. Good agreement between the coefficients can be seen in the V -band $[\text{Fe}/\text{H}]-\phi_{31}-P$ relation derived in [Mullen et al. \(2021\)](#) and in our work, suggesting the V -band $[\text{Fe}/\text{H}]-\phi_{31}-P$ relation is robust, no matter it is derived from an “all-sky” sample as done in [Mullen et al. \(2021\)](#), with $\sim 10^3$ ab-type RR Lyrae or from a “local” sample of 30 ab-type RR Lyrae located in the *Kepler* field. Furthermore, the V -band light-curves are totally independent in these works. Together with the infra-red $[\text{Fe}/\text{H}]-\phi_{31}-P$ relation presented in [Mullen et al. \(2021\)](#), i.e. $[\text{Fe}/\text{H}]_{\text{WISE}} = -1.47 - 8.33(P - 0.58) + 0.92(\phi_{31} - 1.90)$, we found that both period coefficient (b) and ϕ_{31} coefficient (c) in the $[\text{Fe}/\text{H}]-\phi_{31}-P$ relations monotonically decrease when the wavelength is increasing.

ACKNOWLEDGMENTS

We thank the useful discussions and comments from an anonymous referee to improve the manuscript. We sincerely thank the observing staff at the Lulin Observatory, C.-S. Lin, H.-Y. Hsiao, and W.-J. Hou, to carry out the queue observations for this work. We are thankful for funding from the Ministry of Science and Technology (Taiwan) under the contract 109-2112-M-008-014-MY3. This research made use of [Astropy](#),⁶ a community-developed core Python package for Astronomy ([Astropy Collaboration et al. 2013, 2018](#)). This research has made use of the VizieR catalogue access tool, CDS, Strasbourg, France. The original description of the VizieR service was published in [Ochsenbein et al. \(2000\)](#).

The Pan-STARRS1 Surveys (PS1) and the PS1 public science archive have been made possible through contributions by the Institute for Astronomy, the University of Hawaii, the Pan-STARRS Project Office, the Max-Planck Society and its participating institutes, the Max Planck Institute for Astronomy, Heidelberg and the Max Planck Institute for Extraterrestrial Physics, Garching, The Johns Hopkins University, Durham University, the University of Edinburgh, the Queen’s University Belfast, the Harvard-Smithsonian Center for Astrophysics, the Las Cumbres Observatory Global Telescope Network Incorporated, the National Central University of Taiwan, the Space Telescope Science Institute, the National Aeronautics and Space Administration under Grant No. NNX08AR22G issued through the Planetary Science Division of the NASA Science Mission Directorate, the National Science Foundation Grant No. AST-1238877, the University of Maryland, Eotvos Lorand University (ELTE), the Los Alamos National Laboratory, and the Gordon and Betty Moore Foundation.

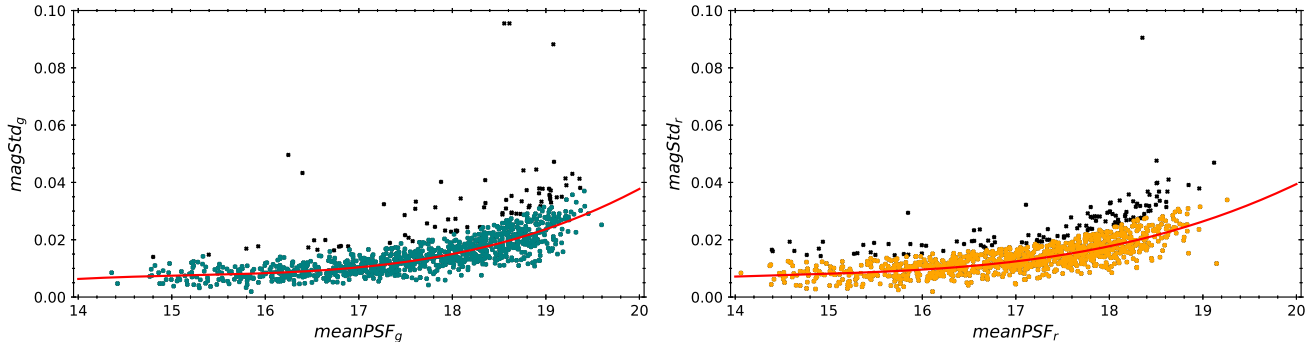


Figure 6. An example of the plots of $magStd$ vs. $meanPSF$ in the g - and r -band, shown in the left and right panel, respectively, for KIC12155928. The black points are the rejected data points after the initial fitting with a 3rd-degree polynomial function. The polynomial function was applied again to fit the remaining data points (in various colors) in the second step of the two-steps fitting procedure, and displayed as the red curves. Only the data points below the red curves were selected as reference stars. All data points were extracted from the Pan-STARRS1 DR1 photometric catalogs.

Software: `astropy` (Astropy Collaboration et al. 1996), `Matplotlib` (Hunter 2007), `NumPy` (Harris et al. 2013, 2018), `astrometry.net` (Lang et al. 2010), `IRAF` (Tody 1986, 1993), `SExtractor` (Bertin & Arnouts 2020), `SciPy` (Virtanen et al. 2020).

APPENDIX

A. SELECTION OF REFERENCE STARS

We summarize a number of selection criteria to select non-varying stellar sources from the catalogs merged with Pan-STARRS1 DR1 photometric catalog and the UBV photometric catalog given in Everett et al. (2012). These non-varying stellar sources will be used to construct a reference stars catalog for each of the targeted RR Lyrae. The selection criteria are listed below, some of them were inspired from, or similar to those adopted in, the ZTF Science Data System Explanatory Supplement.⁷

- Excluding the targeted RR Lyrae.
- Separation of the matched sources when cross-matching the Pan-STARRS1 DR1 and the UBV catalogs is smaller than $1''$.
- Sources without measurements in any of the $BVgri$ bands in the merged catalogs were excluded.
- Sources with number of observations in each of the gri -band is greater than 5.
- Sources with mean PSF magnitudes ($meanPSF$) in gri -band that are in between 14 mag and 20 mag.
- Sources with difference between the i -band mean PSF magnitudes and mean Kron magnitudes ($meanKron$), $meanPSF_i - meanKron_i$, that are within the range of -1.5 mag and -0.04 mag.
- Sources with color, $meanPSF_g - meanPSF_i$, that are within the range of -0.5 mag and 3.0 mag.
- Sources with photometric errors in all of the $BVgr$ bands that are smaller than 0.1 mag.
- Sources with standard deviations ($magStd$) in the gr -band $meanPSF$ that are smaller than 0.1 mag.

For the remaining sources after applying the above selection criteria, a 3rd-degree polynomial function was fitted to the gr -band $meanPSF$ and $magStd$ in a two-steps process. In the first step, we removed data points that were larger

⁷ See https://irsa.ipac.caltech.edu/data/ZTF/docs/ztf_explanatory_supplement.pdf

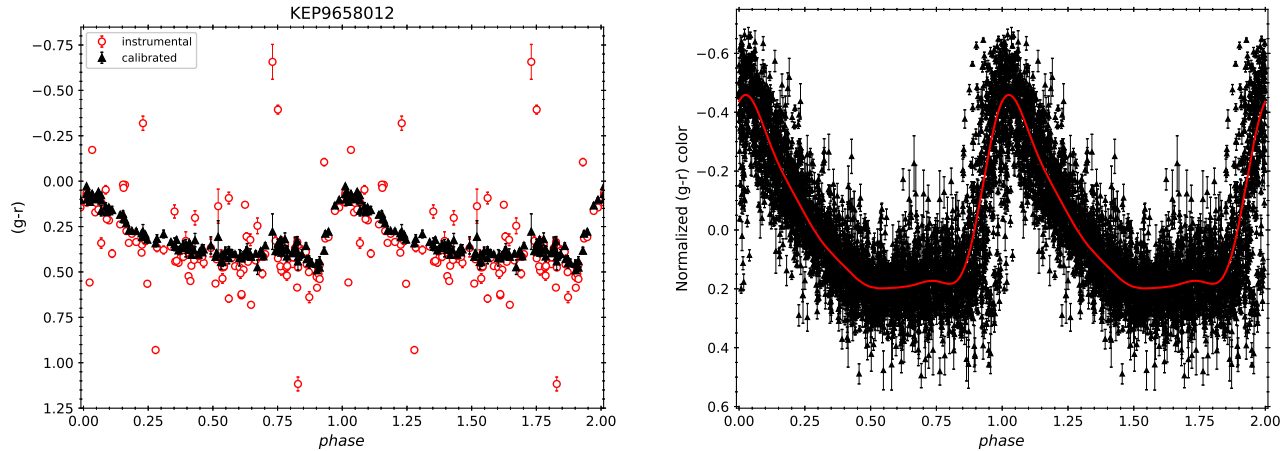


Figure 7. Left panel: Comparison of the instrumental ($g^{\text{instr}} - r^{\text{instr}}$) colors (in red open circles) and the calibrated ($g^{PS1} - r^{PS1}$) colors (in black filled triangles), using equation (6), for the same RR Lyrae as presented in Figure 1. **Right panel:** Composite of the normalized ($g - r$) color-curve based on 27 RR Lyrae (excluding KIC 3864443, 4484128, and 7198959; due to larger scatters seen on their color-curves), the red curve represents the best-fit template color-curve (see text for details).

than 1 standard deviation from the best-fit polynomial function. The rest of the data points were re-fit in the second step of the process (see Figure 6). We only retained sources that have *magStd* smaller than the best-fit polynomial function in both *gr*-band as reference stars for performing the photometric calibration (see Section 3). The number of the selected reference stars varies from ~ 160 to ~ 1120 for the 30 targeted RR Lyrae.

B. COLOR-CURVE TEMPLATE

The near simultaneous *gr*-band observations of our targeted RR Lyrae allow the construction of color-curves via equation (6), an example is presented in the left panel of Figure 7. These color-curves can be used to construct a template color-curve in the ($g - r$) color. We first removed data points with errors larger than 0.1 mag (they tend to be outliers on the color-curves), and then normalized the color-curves by subtracting the means and scaled with their amplitudes. Finally, we re-phased the color-curves using the reference epoch t_0 adopted from Nemec et al. (2013, their Table 1). The composite color-curve is presented in the right panel of Figure 7, and fitted with a low-order Fourier sine series. The best-fit template color-curve, shown as red curve in the right panel of Figure 7, is:

$$c(\Phi) = 0.280 \sin(2\pi\Phi + 4.205) + 0.111 \sin(4\pi\Phi + 4.088) + 0.062 \sin(6\pi\Phi + 4.430), \\ + 0.027 \sin(8\pi\Phi + 4.808) + 0.011 \sin(10\pi\Phi + 5.138), \quad (\text{B1})$$

with an RMS of 0.131, where $c = (g - r)$.

REFERENCES

- Aihara, H., Arimoto, N., Armstrong, R., et al. 2018, PASJ, 70, S4
- Allcock, C., Allsman, R. A., Alves, D. R., et al. 2000, AJ, 119, 2194
- Astropy Collaboration, Robitaille, T. P., Tollerud, E. J., et al. 2013, A&A, 558, A33
- Astropy Collaboration, Price-Whelan, A. M., Sipőcz, B. M., et al. 2018, AJ, 156, 123
- Beaton, R. L., Bono, G., Braga, V. F., et al. 2018, SSRv, 214, 113
- Bellm, E. C., Kulkarni, S. R., Graham, M. J., et al. 2019, PASP, 131, 018002
- Bertin, E. & Arnouts, S. 1996, A&AS, 117, 393
- Bhardwaj, A. 2020, Journal of Astrophysics and Astronomy, 41, 23
- Carretta, E., Bragaglia, A., Gratton, R., et al. 2009, A&A, 508, 695
- Chambers, K. C., Magnier, E. A., Metcalfe, N., et al. 2016, arXiv:1612.05560

- Crestani, J., Fabrizio, M., Braga, V. F., et al. 2021, *ApJ*, 908, 20
- Dark Energy Survey Collaboration, Abbott, T., Abdalla, F. B., et al. 2016, *MNRAS*, 460, 1270
- Deb, S. & Singh, H. P. 2009, *A&A*, 507, 1729
- Dékány, I., Grebel, E. K., & Pojmański, G. 2021, *ApJ*, 920, 33
- Everett, M. E., Howell, S. B., & Kinemuchi, K. 2012, *PASP*, 124, 316
- Fabrizio, M., Braga, V. F., Crestani, J., et al. 2021, *ApJ*, 919, 118
- Flewelling, H. A., Magnier, E. A., Chambers, K. C., et al. 2020, *ApJS*, 251, 7
- Graham, M. J., Kulkarni, S. R., Bellm, E. C., et al. 2019, *PASP*, 131, 078001
- Harris, C. R., Millman, K. J., van der Walt, S. J., et al. 2020, *Nature*, 585, 357
- Hernitschek, N. & Stassun, K. G. 2022, *ApJS*, 258, 4
- Hunter, J. D. 2007, *Computing in Science and Engineering*, 9, 90
- Iorio, G. & Belokurov, V. 2021, *MNRAS*, 502, 5686
- Ivezić, Ž., Kahn, S. M., Tyson, J. A., et al. 2019, *ApJ*, 873, 111
- Jurcsik, J. & Kovacs, G. 1996, *A&A*, 312, 111
- Lang, D., Hogg, D. W., Mierle, K., et al. 2010, *AJ*, 139, 1782
- Martinez-Vazquez, C. E., Monelli, M., Bono, G., et al. 2016, *Communications of the Konkoly Observatory Hungary*, 105, 53
- Masci, F. J., Laher, R. R., Rusholme, B., et al. 2019, *PASP*, 131, 018003
- Morgan, S. M., Wahl, J. N., & Wieckhorst, R. M. 2007, *MNRAS*, 374, 1421
- Mullen, J. P., Marengo, M., Martínez-Vázquez, C. E., et al. 2021, *ApJ*, 912, 144
- Nemec, J. M., Smolec, R., Benkő, J. M., et al. 2011, *MNRAS*, 417, 1022
- Nemec, J. M., Cohen, J. G., Ripepi, V., et al. 2013, *ApJ*, 773, 181
- Ngeow, C.-C., Yu, P.-C., Bellm, E., et al. 2016, *ApJS*, 227, 30
- Ngeow, C.-C., Bhardwaj, A., Dekany, R., et al. 2022, *AJ*, 163, 239
- Ochsenbein, F., Bauer, P., & Marcout, J. 2000, *A&AS*, 143, 23
- Oluseyi, H. M., Becker, A. C., Culliton, C., et al. 2012, *AJ*, 144, 9
- Onken, C. A., Wolf, C., Bessell, M. S., et al. 2019, *PASA*, 36, e033
- Petersen, J. O. 1986, *A&A*, 170, 59
- Petersen, J. O. 1994, *A&AS*, 105, 145
- Sandage, A. 2004, *AJ*, 128, 858
- Sandage, A. & Tammann, G. A. 2006, *ARA&A*, 44, 93
- Sesar, B., Ivezić, Ž., Grammer, S. H., et al. 2010, *ApJ*, 708, 717
- Simon, N. R. & Lee, A. S. 1981, *ApJ*, 248, 291
- Smolec, R. 2005, *Acta Astronomica*, 55, 59
- Tody, D. 1986, *Proc. SPIE*, 627, 733
- Tody, D. 1993, *Astronomical Data Analysis Software and Systems II*, 52, 173
- Tonry, J. L., Stubbs, C. W., Lykke, K. R., et al. 2012, *ApJ*, 750, 99
- Virtanen, P., Gommers, R., Oliphant, T. E., et al. 2020, *Nature Methods*, 17, 261
- Watkins, L. L., Evans, N. W., Belokurov, V., et al. 2009, *MNRAS*, 398, 1757
- Wu, C., Qiu, Y. L., Deng, J. S., et al. 2006, *A&A*, 453, 895